A Novel Ferroptosis-related 6-Gene Signature for Overall Survival Prediction in Patients with Thyroid carcinoma

Zhixing Wang
The First Affiliated Hospital of Shantou University Medical College
Fudan Qiu
The First Affiliated Hospital of Shantou University Medical College
Peilin Shen (plshen@stu.edu.cn)
The First Affiliated Hospital of Shantou University Medical College https://orcid.org/0000-0003-3584-3449

Research

Keywords: thyroid carcinoma, Ferroptosis, TCGA database, overall survival

Posted Date: April 8th, 2021

DOI: https://doi.org/10.21203/rs.3.rs-391766/v1

Abstract

Background: Ferroptosis is a new form of regulated cell death (RCD) that plays a crucial role in the genesis and prognosis of tumor. Nevertheless, the relationship between ferroptosis and the prognosis of thyroid carcinoma (THCA) remains unclear and needs to be explored.

Methods: By analyzing data from the THCA cohort in the TCGA database, ferroptosis-related differentially expressed genes (DEGs) with prognostic value were identified, which were used to establish a prognostic signature based on Lasso-penalized Cox regression analysis. Then, the model was testified with Kaplan-Meier survival, Cox regression and receiver operating characteristic (ROC) analyses based on overall survival (OS). Finally, DEGs between the low-risk and high-risk groups were identified and used to conduct GO enrichment analysis, KEGG pathways analysis and immune infiltration analysis.

Results: A 6-gene signature was constructed which including DPP4, GPX4, GSS, HMGCR, TFRC and PGD. The area under the curve (AUC) were 0.890 (1 year), 0.863 (2 years) and 0.883 (3 years) which validated the prominent predictive capacity of the model. Multivariate Cox regression certified the model as a prognostic-related independent predictor for OS.

Conclusion: In this study, we established an innovative prognostic signature of 6 ferroptosis-related genes which can be as a prognostic-related independent predictor for OS in THCA, while the potential mechanisms was still unclear and needed further exploration.

Background

Thyroid carcinoma (THCA) is one of the most common malignant head and neck tumors. Over the past several decades, the morbidity of thyroid cancer has been increasing and it is expected to be the fourth most common diagnostic cancer in the world [1]. Thyroid carcinoma can be classified into several subtypes: differentiated thyroid cancer (including papillary, follicular and Hürthle cell), medullary thyroid cancer and anaplastic thyroid cancer [2]. Among them, papillary thyroid carcinoma (PTC) is the most common type which accounting for more than 80% of reported cases[3]. The traditional treatment of THCA includes surgical therapy, radioactive iodine (RAI), chemotherapy and thyroxine therapy [4, 5]. Although the prognosis of most patients with traditional therapy is excellent, there were still some patients with high mortality, including undifferentiated, recurrent and metastatic thyroid cancer [5]. Thus, it is necessary to search for new molecular targets for detection and early intervention for THCA with poor prognosis.

Ferroptosis, a new kind of regulated cell death (RCD), is distinct from other cell death patterns such as necroptosis, apoptosis and autophagy in morphology and biochemistry. It is defined as an iron-catalyzed form of RCD caused by unrestricted lipid peroxidation and subsequent membrane damage [6, 7]. Iron accumulation and lipid peroxidation are the two main biochemical characteristics of Ferroptosis [8]. Recently, numerous of studies have shown that ferroptosis is involved in the pathological process of many diseases, such as brain injury, renal disease, liver diseases and many kinds of cancer [9–13].

Reports have indicated that the regulatory mechanisms of ferroptosis may involve the GPX4, SLC7A11, p53 and Non-Coding RNAs [14]. Meanwhile, more and more ferroptosis-related genes have been found, and scientists were keen on exploring the function of ferroptosis-related genes in cancer in order to find more biological factors with diagnostic, prognostic or therapeutic value. Liang et al. structured and validated a signature of ferroptosis-related genes for overall survival (OS) to predict the prognosis of hepatocellular cancer patients [15]. Another study [16] suggested that low expression of ferroptosis-related NCOA4 gene was associated with poor prognosis, disease progression and impaired infiltration of immune cells in clear cell renal carcinoma. However, few studies focused on the role of ferroptosis in malignant tumor of endocrine-system, especially thyroid cancer.

In our study, we sought to explore the potential relationships between ferroptosis and THCA prognosis based on the Cancer Genome Atlas (TCGA) datasets. We identified prognostic ferroptosis-related genes and structured a ferroptosis-related gene model for OS. Then, bioinformatics analyses were performed to explore the potential mechanism. This study can offer potential clinical utility of ferroptosis and great promise for prognosis prediction and targeted therapy of THCA.

Materials And Methods

Retrieving mRNA sequencing and corresponding clinical data

MRNA sequencing data (HTSeq-FPKM) and corresponding clinical information of THCA and normal thyroid tissue samples were downloaded from the THCA cohort in the TCGA database (https://portal.gdc.cancer.gov/) up to December 5, 2020 using the “TCGAbiolinks” R package [17]. Then the scale method form the "limma" R package [18] was used to normalize the gene expression profiles. No ethical approval from local ethics committees was required because all the data utilized in our study were obtained from public database.

Construction and further analysis of the prognostic ferroptosis-related gene model.

60 ferroptosis-related genes (provided in Supplementary Table S1) were obtained from the high-quality articles gathered by the comprehensive literature survey [14, 19–21], in which differentially expressed genes (DEGs) between the THCA tissues and non-tumorous tissues were identified with a $|\log2FC| \geq 1$ and false discovery rate (FDR) < 0.05 using the "limma" R package. Prognostic ferroptosis-related DEGs were screened out using the univariate Cox analysis of OS. LASSO Cox regression analysis was used to establish a prognostic ferroptosis-related gene model with the "glmnet" R package [22–24]. Based on the prognostic model, all patients were assigned with risk scores according to the established score formula (risk score = sum (expression level of each gene * corresponding coefficient) and grouped into low-risk group or high-risk group by comparing to the median risk score. Next, principal component analysis (PCA) and t-distributed stochastic neighbor embedding (t-SNE) analysis were performed to show the distribution of patients. The Kaplan-Meier survival analysis and the receiver operating characteristic (ROC) curve were

used to evaluate the predictive value of OS for the signature and the Cox analyses was conducted to identify the independent predictive factor. Following, Gene Ontology (GO) and Kyoto Encyclopedia of Genes and Genomes (KEGG) analyses were performed by the "clusterProfiler" R package [25] (*P*-value < 0.05, gene count > 10) based on the DEGs between the low-risk and high-risk group (|log2FC| ≥ 1, FDR < 0.05). We used single sample gene set enrichment analysis (ssGSEA) [26] to calculated the normalized enrichment scores of 16 immune-related cells and 13 immune-related pathways (the annotated gene sets file was provided in Supplementary Table S2) with the "gsva" R package [27] in order to explore the correlation between immune status and risk score. At last, using the immunohistochemistry images from the human protein atlas (HPA) database (http://www.proteinAtlas.org/), we analyzed protein expression levels of the genes in the signature. And the cbioProtal database (http://www.cbioportal.org/) was accessed to analyze the genetic alteration of these genes.

Statistical analysis

All statistical analyses and most of visualization were performed in the R (version 4.0.3) and the SPSS software (version 22.0). Univariate Cox analysis was conducted to identify prognostic genes for OS. We used the LASSO Cox regression analysis to calculate the risk coefficient of each gene and construct the prognostic model. Difference of clinical data between the low-risk and high-risk group were analysed by Chi square test. Univariate and multivariate Cox analyses were performed to find the independent predictive factor. The ssGSEA was utilized to quantify the THCA samples and Mann–Whitney U tests was used to compare the ssGSEA scores between the low-risk and high-risk group. A *P* value less than 0.05 indicated statistical significance.

Results

Study population and data acquisition

The detailed workflow of this study is shown in Fig. 1. 497 THCA samples and 56 normal tissue samples were retrieved, and the clinical characteristics of which were showed in Table 1.

Table 1
Clinical characteristics of the patients in the present study

Clinical characteristics	Variable	Total
Gender	Female	367(73.1%)
	Male	135(26.9%)
Stage	I	281(56.0%)
	II	52(10.4%)
	III	112(22.3%)
	IV	55(11.0%)
	unknown	2(0.4%)
T	T1	143(28.5%)
	T2	164(32.7%)
	T3	170(33.9%)
	T4	23(4.6%)
	TX	2(0.4%)
N	N0	229(46.5%)
	N1	223(44.4%)
	NX	50(10.0%)
M	M0	282(56.2%)
	M1	9(1.8%)
	MX	210(41.8%)
Survival status	Dead	16(3.2%)
	Alive	486(96.8%)
Age (median, range)		48(15–90)

Identification of prognostic DEGs related to THCA and ferroptosis

We found 44 DEGs from 60 ferroptosis-related genes obtained from previous published literatures, in which DPP4, GPX4, GSS, HMGCR, TFRC, SQLE and PGD were significantly related to OS according to univariate Cox regression (Fig. 2a and 2b). The expression of 7 genes between different tissues were displayed with heat map in Fig. 2c. Forest plots (Fig. 2a) of OS showed that HMGCR, TFRC, SQLE and

PGD were the high-risk genes, while DPP4, GPX4 and GSS were the protective genes for THCA. The correlation network in Fig. 2d shown the correlation between the prognostic DEGs related to ferroptosis.

Construction of a prognostic ferroptosis-related 6-gene signature

Based on the LASSO Cox regression analysis, we used the 7 OS-associated genes above to constructed a prognostic gene signature. A 6-gene signature was established and the coefficients of each gene within are list in Table 2. Each patient's risk score was calculated from each gene's expression and regression coefficients as follows: Risk score = (-0.33121 * expression value of DPP4) + (0.92445 * expression level of GPX4) + (-2.62370 * expression level of GSS) + (0.08964 * expression level of HMGCR) + (1.08994 * expression level of TFRC) + (0.85750 * expression level of PGD). We classified all patients into the low- or high-risk group according to the corresponding risk scores (Fig. 3a). The difference of clinical data between the two groups were shown in Table 3 and we found that the low-risk group had better OS. PCA (Fig. 3b) and t-SNE (Fig. 3c) analysis shown that patients in this two risk groups were divided into two diverse sets. The dead cases were mainly distributed in the high-risk group (Fig. 3d). The Kaplan–Meier cumulative curve displayed that a patient with high risk score had a significantly worse survival outcome than those with low risk score (Fig. 3e). Next, we used the ROC curve (Fig. 3f) to evaluate the prognostic value of the model. The area under the curve (AUC) from the ROC analysis were 0.890 (1 year), 0.863 (2 years) and 0.883 (3 years), which indicated this model as a highly reliable prognosic predictor.

Table 2
Baseline characteristics of the patients in different risk groups

Characteristics		Low risk	High risk	*P* value
Age	≤65	218(87.9%)	202(81.5%)	0.046
	>65	30(12.1%)	46(18.5%)	
Gender	Female	166(66.9%)	196(79.0%)	0.002
	Male	82(33.1%)	52(21.0%)	
T	T1	65(26.2%)	76(30.6%)	0.211
	T2	74(29.8%)	88(35.5%)	
	T3	94(37.9%)	75(30.2%)	
	T4	14(5.6%)	8(3.2%)	
	TX	1(0.4%)	1(0.4%)	
N	N0	106(42.7%)	121(48.8%)	0.038
	N1	123(49.6%)	97(39.1%)	
	NX	19(7.7%)	30(12.1%)	
M	M0	147(59.3%)	135(54.4%)	0.290
	M1	2(0.8%)	6(2.4%)	
	MX	99(39.9%)	107(43.2%)	
Stage	I	133(53.8%)	146(59.1%)	0.058
	II	20(8.1%)	32(13.0%)	
	III	62(25.1%)	48(19.4%)	
	IV	32(13.0%)	21(8.5%)	
Survival status	Dead	2(0.8%)	14(5.6%)	0.002
	Alive	246(99.2%)	234(94.4%)	

Table 3
The coefficients of each gene in prognostic model

Gene symbol	Full name	Coefficient
DPP4	dipeptidyl peptidase 4	-0.331212959
GPX4	glutathione peroxidase 4	0.924455134
GSS	glutathione synthetase	-2.623701778
HMGCR	3-hydroxy-3-methylglutaryl-CoA reductase	0.089643927
TFRC	transferrin receptor	1.089946091
PGD	phosphogluconate dehydrogenase	0.857505774

Independent predictive factor for THCA prognosis

Univariate and multivariate Cox analyses were used to test and verify whether the risk score in this model can be as an independent predictive factor for THCA prognosis from other factors such as age, gender and clinical stage. The forest plot (Fig. 4a) of univariate Cox regression analysis displayed that stage, age, and risk score (HR = 2.996, 95% CI = 2.014–4.458, $P < 0.001$) were related to OS in THCA patients. The multivariate Cox analysis (Fig. 4b) confirmed that risk score (HR = 2.048, 95% CI = 1.395–3.006, $P < 0.001$) and age can be as independent predictive factors for OS in the THCA patients.

Functional enrichment analysis and immune-related analysis in the THCA cohort

To investigate the biological characteristics of the prognostic signature, we identified the DEGs between the low-risk and high-risk group, which were used to conducted GO and KEGG functional analyses. The top 10 enriched terms in GO and top 16 enriched terms in KEGG were shown in Fig. 5a and Fig. 5b. From the result of GO, we found out that the DEGs were enriched in several biological process (BP) terms such as hormone metabolic process, organic acid transport, stress response to metal ion, stress response to copper ion and response to cadmium ion. The main enriched cellular component (CC) term includes collagen – containing, extracellular matrix, specific granule lumen. In addition, the DEGs are also enriched in several molecular function (MF) term, such as carboxylic acid binding and organic acid binding. KEGG analysis demonstrated that the DEGs were related to thyroid hormone synthesis, mineral absorption, pancreatic secretion and gastric acid secretion. Interestingly, we can find that many hormone-metabolic-related process (especially thyroid hormone), organic-acid-related process (especially fatty acid and carboxylic acid) and ion-related process were enriched.

In order to analyze the relationship between immunology and THCA, ssGSEA was performed to quantify the enrichment scores of the immune cells and the immune-related pathways between the low- and high-risk group in THCA samples. For immune cells, the result (Fig. 5c) showed that the score of natural killer cells (NK-cells), mast-cells, dendritic cells (DCs), immature DCs (iDCs), activated DCs (aDCs) and in the

low-risk group were significantly higher than those in the high-risk group. Interestingly, for immune-related functions and pathways (Fig. 5d), the score of antigen-presenting cell (APC) co-stimulation, APC co-inhibition, MHC class I, parainflammation, type-I immune interferon (IFN) reponse, check – point and human leukocyte antigen (HLA) had similar conditions.

Comprehensive analysis of 6 genes in prognostic signature

Finally, we further explored the biological characteristics of the genes in the prognostic signature. The HPA database was used to evaluated the protein expression. As shown in the immunohistochemistry images (Fig. 6a), the protein expression levels of most genes were basically consistent with the mRNA levels. The cBioPortal database was accessed to analyze the genetic alteration of these genes. The results showed (Fig. 6b) that DDP4 and GSS has the highest alteration frequency (8% and 7%). GPX4 and HMGCR has the same alteration ratio of 6%. While the mutations ratio of PGD (5% of all sample) and TFRC (4% of all sample) was relatively lower than others. Meanwhile, we observed that the major type of alteration were mRNA expression changes, which may be an important prognostic factor for THCA.

Discussion

For the last several decades, the morbidity of thyroid carcinoma has been increasing in the world. Although the traditional therapy can cure most patients, there are still some THCA patients suffer from poor prognosis, which encourage scientist to continue to explore the new targets for prognosis prediction and treatment. Ferroptosis, an iron-dependent and non-apoptotic RCD process, has been proved by many researches that it is playing an important role in several cancers [28], especially in terms of diagnosis and prognosis. Nevertheless, the biological value of ferroptosis in THCA have not been systematically explored by far. Here, our study first identified the prognostic ferroptosis-related genes and structured a 6-gene signature for OS based on THCA dataset. Further biological analysis helped us to explore the potential mechanism of ferroptosis in THCA and we found that hormone and immune function may be valuable for further research.

The Kaplan-Meier analysis and ROC curve showed that the prognostic model we structured provided an excellent predictive value for OS. The prognostic signature was made up of 6 ferroptosis-related genes (DPP4, GPX4, GSS, HMGCR, TFRC and PGD). P53 gene is a well-known tumor suppressor gene, the oncosuppressive functions of which have been proved to be influenced by ferroptosis [29, 30]. A recent study [31] found that nuclear accumulation of DPP4 can be prohibited due to the loss of P53 which will promote DPP4-dependent lipid peroxidation and finally lead to ferroptosis. GPX4 is a glutathione (GSH) dependent enzyme which can catalyses and reduces lipid peroxides [32]. While, ferroptosis inducers can impair the GSH, resulting in excessive aggregation of lipid ROS and finally leading to cell death [33]. A study found that the overexpression and knockdown of GPX4 can modulate the lethality of 12 ferroptosis inducers which proved that GPX4 was the important regulator of ferroptosis [34]. GSS is also associated with GSH, which inhibited elevated lipid ROS levels in HepG2 cells [35]. In addition, another study shown that ribonucleotide reductase regulatory subunit M2 (RRM2) inhibited ferroptosis by stimulating GSH synthesis via GSS in liver cancer [36]. Sterols coenzyme Q10 (CoQ10) is an inhibited of ferroptosis, the

synthesis of which can be regulated by HMGCR through regulating the synthesis of mevalonic acid. Shimada et al. [37] found that the inhibition of HMGCR can enhances FIN-56-induced ferroptosis. TFRC, takes part in cellular transferrin-iron uptake, with other ferroptosis modulators can be upregulated by proto-oncogenic transcriptional co-activator YAP which result in promoting ferroptosis [38, 39]. For PGD, a kind of pentose phosphate pathway (PPP) enzymes, have been found that the knockdown of which suppressed erastin-induced ferroptosis in Calu-1 cell of non-small cell lung cancer[6]. To sum up, 3 genes (DPP4, TFRC and PGD) in prognostic signature were confirmed to promot ferroptosis, while the other 3 genes (GPX4, GSS and HMGCR) can protect cells from ferroptosis. Though the prognostic model we structured performed an excellent predictive value for OS and these 6 genes were proved as ferroptosis-related genes, whether these genes influence the prognosis of THCA by regulating and controlling the process of ferroptosis remains to be verified.

In order to explore the potential mechanism, we further conducted GO and KEGG analyses and found that several organic-acid-related terms and ion-related terms were significantly enriched. Interestingly, GO and KEGG analyses both pointed out that the risk-related DEGs was correlated with hormone-metabolic-related process, especially thyroid hormone. Weigand et al. found that adrenal cortex cells are extraordinary sensitive to ferroptosis which depend on the active steroid synthetic pathways [40]. Another study [41] found that melatonin may be an excellent ferroptosis inhibitor and it can produce cerebroprotection from traumatic brain injury (TBI) by inhibiting neuronal Fth-mediated ferroptosis. These previous researches indicated that diseases can be affected by hormone through ferroptosis-related pathways. Though we have not found any report about the correlation between thyroid hormone and ferroptosis, it is reasonable to assume that thyroid hormone synthesis can affect the prognosis of THCA by influencing the process of ferroptosis.

As is known to all, our immune system plays a vital role in the development of cancer. Ferroptosis and immunoregulation are both intense research areas in oncology, and they can provide different elimination mechanisms for cancer cells. Nevertheless, the relationship between ferroptosis and tumor immunity remains elusive. In our study, we found that the ssGSEA scores of several immune-related cell and functions were significantly lower in the high-risk group, including Type_I_IFN_Reponse, MHC_class_I, APC_co_stimulation and the NK_cells. Thus, immune escape may be an important reason for the poorly prognosis of the THCA patients in the high-risk group, which may be affected by ferroptosis. A recent research pointed out that ferroptotic cancer cells can be engulfed by macrophages in vitro [42]. This process may correlate with the modulation of antitumour immunity by AA oxidation products released from ferroptotic cells. In addition, cancer cells can be recognized by NK cells and its antigens will be presented to T cells through other immune cells and immune factors, which will eventually lead to cell elimination by the immune system [43, 44]. A speculation about ferroptosis pointed out that ferroptotic cells can release signals which can attract the APCs or other immune cells to the location where the ferroptotic cells died [45].

The present study inevitably has several limitations. Firstly, this is a retrospective study because all the mRNA sequencing data were from TCGA database and no prospective validation in a clinical trial was

conducted. What's more, we failed to find a validation dataset for our model from other databases. Lastly, the underlying mechanisms of ferroptosis-related genes to predict prognosis of thyroid carcinoma are lack of literature support and need to be further investigated.

In sum, we established an innovative independently prognostic model of 6 ferroptosis-related genes based on OS for THCA. Also, our study offered some ideas for further research of the relationship between ferroptosis and thyroid carcinoma, especially in hormone and immune function.

Abbreviations

aDCs activated dendritic cells

APC antigen-presenting cell

AUC area under the curve

BP biological process

CC cellular component

CoQ10 coenzyme Q10

DCs dendritic cells

DEGs differentially expressed genes

FDR false discovery rate

GO Gene Ontology

GSH glutathione

HPA human protein atlas

iDCs immature dendritic cells

IFN Interferon

KEGG Kyoto Encyclopedia of Genes and Genomes

MF molecular function

OS overall survival

PCA principal component analysis

PPP pentose phosphate pathway

PTC papillary thyroid carcinoma

RAI radioactive iodine

RCD regulated cell death

ROC receiver operating characteristic

RRM2 ribonucleotide reductase regulatory subunit M2

ssGSEA single sample gene set enrichment analysis

TBI traumatic brain injury

TCGA the Cancer Genome Atlas

THCA Thyroid carcinoma

t-SNE t-distributed stochastic neighbor embedding

Declarations

Ethics approval and consent to participate

Not applicable

Consent for publication

Not applicable

Data Availability

The data analyzed for the present study can be found in the TCGA database (https://portal.gdc.cancer.gov/). The other data supporting the findings of this study are available within the article and its supplementary information files.

Competing interests

The authors declare that they have no competing interests.

Funding

None.

Authors' contributions

Z.x.W. and P.l.S. designed the present study. Z.x.W. and F.d.Q completed the search and downloaded the data. Z.x.W. and P.l.S. analyzed the data and designed the illustrations. Z.x.W. wrote the manuscript. All authors read and approved the final manuscript.

Acknowledgements

Not applicable

References

1. Kim J, Gosnell JE, Roman SA. **Geographic influences in the global rise of thyroid cancer**. 2020, 16:17–29.
2. Haddad RI, Nasr C, Bischoff L, Busaidy NL, Byrd D, Callender G, Dickson P, Duh QY, Ehya H, Goldner W, et al. NCCN Guidelines Insights: Thyroid Carcinoma, Version 2.2018. J Natl Compr Canc Netw. 2018;16:1429–40.
3. Schneider DF, Chen H. New developments in the diagnosis and treatment of thyroid cancer. CA Cancer J Clin. 2013;63:374–94.
4. Haugen BR, Alexander EK, Bible KC, Doherty GM, Mandel SJ, Nikiforov YE, Pacini F, Randolph GW, Sawka AM, Schlumberger M, et al. 2015 American Thyroid Association Management Guidelines for Adult Patients with Thyroid Nodules and Differentiated Thyroid Cancer: The American Thyroid Association Guidelines Task Force on Thyroid Nodules and Differentiated Thyroid Cancer. Thyroid. 2016;26:1–133.
5. Glaser SM, Mandish SF, Gill BS, Balasubramani GK, Clump DA, Beriwal S. Anaplastic thyroid cancer: Prognostic factors, patterns of care, and overall survival. Head Neck. 2016;38(Suppl 1):E2083–90.
6. Dixon SJ, Lemberg KM, Lamprecht MR, Skouta R, Zaitsev EM, Gleason CE, Patel DN, Bauer AJ, Cantley AM, Yang WS, et al. Ferroptosis: an iron-dependent form of nonapoptotic cell death. Cell. 2012;149:1060–72.
7. Xie Y, Hou W, Song X, Yu Y, Huang J, Sun X, Kang R, Tang D. Ferroptosis: process and function. Cell Death Differ. 2016;23:369–79.
8. Tang D, Chen X, Kang R, Kroemer G. **Ferroptosis: molecular mechanisms and health implications**.
9. Magtanong L, Dixon SJ. Ferroptosis and Brain Injury. Dev Neurosci. 2018;40:382–95.
10. Ren JX, Sun X, Yan XL, Guo ZN, Yang Y. Ferroptosis in Neurological Diseases. Front Cell Neurosci. 2020;14:218.
11. Martin-Sanchez D, Fontecha-Barriuso M, Martinez-Moreno JM, Ramos AM, Sanchez-Niño MD, Guerrero-Hue M, Moreno JA, Ortiz A, Sanz AB. Ferroptosis and kidney disease. Nefrologia. 2020;40:384–94.
12. Capelletti MM, Manceau H, Puy H. Peoc'h K: **Ferroptosis in Liver Diseases: An Overview**. *Int J Mol Sci* 2020, 21.

13. Ye Z, Liu W, Zhuo Q, Hu Q, Liu M, Sun Q, Zhang Z, Fan G, Xu W, Ji S, et al. Ferroptosis: Final destination for cancer? Cell Prolif. 2020;53:e12761.
14. Hassannia B, Vandenabeele P, Vanden Berghe T. Targeting Ferroptosis to Iron Out Cancer. Cancer Cell. 2019;35:830–49.
15. Liang JY, Wang DS, Lin HC, Chen XX, Yang H, Zheng Y, Li YH. A Novel Ferroptosis-related Gene Signature for Overall Survival Prediction in Patients with Hepatocellular Carcinoma. Int J Biol Sci. 2020;16:2430–41.
16. Mou Y, Wu J, Zhang Y, Abdihamid O, Duan C, Li B. Low expression of ferritinophagy-related NCOA4 gene in relation to unfavorable outcome and defective immune cells infiltration in clear cell renal carcinoma. BMC Cancer. 2021;21:18.
17. Colaprico A, Silva TC, Olsen C, Garofano L, Cava C, Garolini D, Sabedot TS, Malta TM, Pagnotta SM, Castiglioni I, et al. TCGAbiolinks: an R/Bioconductor package for integrative analysis of TCGA data. Nucleic Acids Res. 2016;44:e71.
18. Ritchie ME, Phipson B, Wu D, Hu Y, Law CW, Shi W, Smyth GK. limma powers differential expression analyses for RNA-sequencing and microarray studies. Nucleic Acids Res. 2015;43:e47.
19. Stockwell BR, Friedmann Angeli JP, Bayir H, Bush AI, Conrad M, Dixon SJ, Fulda S, Gascón S, Hatzios SK, Kagan VE, et al. Ferroptosis: A Regulated Cell Death Nexus Linking Metabolism, Redox Biology, and Disease. Cell. 2017;171:273–85.
20. Bersuker K, Hendricks JM, Li Z, Magtanong L, Ford B, Tang PH, Roberts MA, Tong B, Maimone TJ, Zoncu R, et al. The CoQ oxidoreductase FSP1 acts parallel to GPX4 to inhibit ferroptosis. Nature. 2019;575:688–92.
21. Doll S, Freitas FP, Shah R, Aldrovandi M, da Silva MC, Ingold I, Goya Grocin A, Xavier da Silva TN, Panzilius E, Scheel CH, et al. FSP1 is a glutathione-independent ferroptosis suppressor. Nature. 2019;575:693–8.
22. Simon N, Friedman J, Hastie T, Tibshirani R. Regularization Paths for Cox's Proportional Hazards Model via Coordinate Descent. J Stat Softw. 2011;39:1–13.
23. Tibshirani R. The lasso method for variable selection in the Cox model. Stat Med. 1997;16:385–95.
24. Friedman J, Hastie T, Tibshirani R. Regularization Paths for Generalized Linear Models via Coordinate Descent. J Stat Softw. 2010;33:1–22.
25. Yu G, Wang LG, Han Y, He QY. clusterProfiler: an R package for comparing biological themes among gene clusters. Omics. 2012;16:284–7.
26. Rooney MS, Shukla SA, Wu CJ, Getz G, Hacohen N. Molecular and genetic properties of tumors associated with local immune cytolytic activity. Cell. 2015;160:48–61.
27. Hänzelmann S, Castelo R, Guinney J. GSVA: gene set variation analysis for microarray and RNA-seq data. BMC Bioinformatics. 2013;14:7.
28. Shi ZZ, Fan ZW, Chen YX, Xie XF, Jiang W, Wang WJ, Qiu YT, Bai J. Ferroptosis in Carcinoma: Regulatory Mechanisms and New Method for Cancer Therapy. Onco Targets Ther. 2019;12:11291–

304.

29. Jennis M, Kung CP, Basu S, Budina-Kolomets A, Leu JI, Khaku S, Scott JP, Cai KQ, Campbell MR, Porter DK, et al. An African-specific polymorphism in the TP53 gene impairs p53 tumor suppressor function in a mouse model. Genes Dev. 2016;30:918–30.
30. Basu S, Barnoud T, Kung CP, Reiss M, Murphy ME. The African-specific S47 polymorphism of p53 alters chemosensitivity. Cell Cycle. 2016;15:2557–60.
31. Xie Y, Zhu S, Song X, Sun X, Fan Y, Liu J, Zhong M, Yuan H, Zhang L, Billiar TR, et al. The Tumor Suppressor p53 Limits Ferroptosis by Blocking DPP4 Activity. Cell Rep. 2017;20:1692–704.
32. Dolma S, Lessnick SL, Hahn WC, Stockwell BR. Identification of genotype-selective antitumor agents using synthetic lethal chemical screening in engineered human tumor cells. Cancer Cell. 2003;3:285–96.
33. Wang L, Liu Y, Du T, Yang H, Lei L, Guo M, Ding HF, Zhang J, Wang H, Chen X, Yan C. ATF3 promotes erastin-induced ferroptosis by suppressing system Xc. Cell Death Differ. 2020;27:662–75.
34. Yang WS, SriRamaratnam R, Welsch ME, Shimada K, Skouta R, Viswanathan VS, Cheah JH, Clemons PA, Shamji AF, Clish CB, et al. Regulation of ferroptotic cancer cell death by GPX4. Cell. 2014;156:317–31.
35. Jin M, Shi C, Li T, Wu Y, Hu C, Huang G. Solasonine promotes ferroptosis of hepatoma carcinoma cells via glutathione peroxidase 4-induced destruction of the glutathione redox system. Biomed Pharmacother. 2020;129:110282.
36. Yang Y, Lin J, Guo S, Xue X, Wang Y, Qiu S, Cui J, Ma L, Zhang X, Wang J. RRM2 protects against ferroptosis and is a tumor biomarker for liver cancer. Cancer Cell Int. 2020;20:587.
37. Shimada K, Hayano M, Pagano NC, Stockwell BR. Cell-Line Selectivity Improves the Predictive Power of Pharmacogenomic Analyses and Helps Identify NADPH as Biomarker for Ferroptosis Sensitivity. Cell Chem Biol. 2016;23:225–35.
38. Song J, Liu T, Yin Y, Zhao W, Lin Z, Yin Y, Lu D, You F. The deubiquitinase OTUD1 enhances iron transport and potentiates host antitumor immunity. EMBO Rep. 2021;22:e51162.
39. Wu J, Minikes AM, Gao M, Bian H, Li Y, Stockwell BR, Chen ZN, Jiang X. Publisher Correction: Intercellular interaction dictates cancer cell ferroptosis via NF2-YAP signalling. Nature. 2019;572:E20.
40. Weigand I, Schreiner J, Röhrig F, Sun N, Landwehr LS, Urlaub H, Kendl S, Kiseljak-Vassiliades K, Wierman ME, Angeli JPF, et al. Active steroid hormone synthesis renders adrenocortical cells highly susceptible to type II ferroptosis induction. Cell Death Dis. 2020;11:192.
41. Rui T, Wang H, Li Q, Cheng Y, Gao Y, Fang X, Ma X, Chen G, Gao C, Gu Z, et al. Deletion of ferritin H in neurons counteracts the protective effect of melatonin against traumatic brain injury-induced ferroptosis. J Pineal Res. 2021;70:e12704.
42. Klöditz K, Fadeel B. Three cell deaths and a funeral: macrophage clearance of cells undergoing distinct modes of cell death. Cell Death Discov. 2019;5:65.

43. Finn OJ. Immuno-oncology: understanding the function and dysfunction of the immune system in cancer. Ann Oncol. 2012;23(Suppl 8):viii6–9.
44. Kim R, Emi M, Tanabe K. Cancer immunoediting from immune surveillance to immune escape. Immunology. 2007;121:1–14.
45. Friedmann Angeli JP, Krysko DV, Conrad M. Ferroptosis at the crossroads of cancer-acquired drug resistance and immune evasion. Nat Rev Cancer. 2019;19:405–14.

Figures

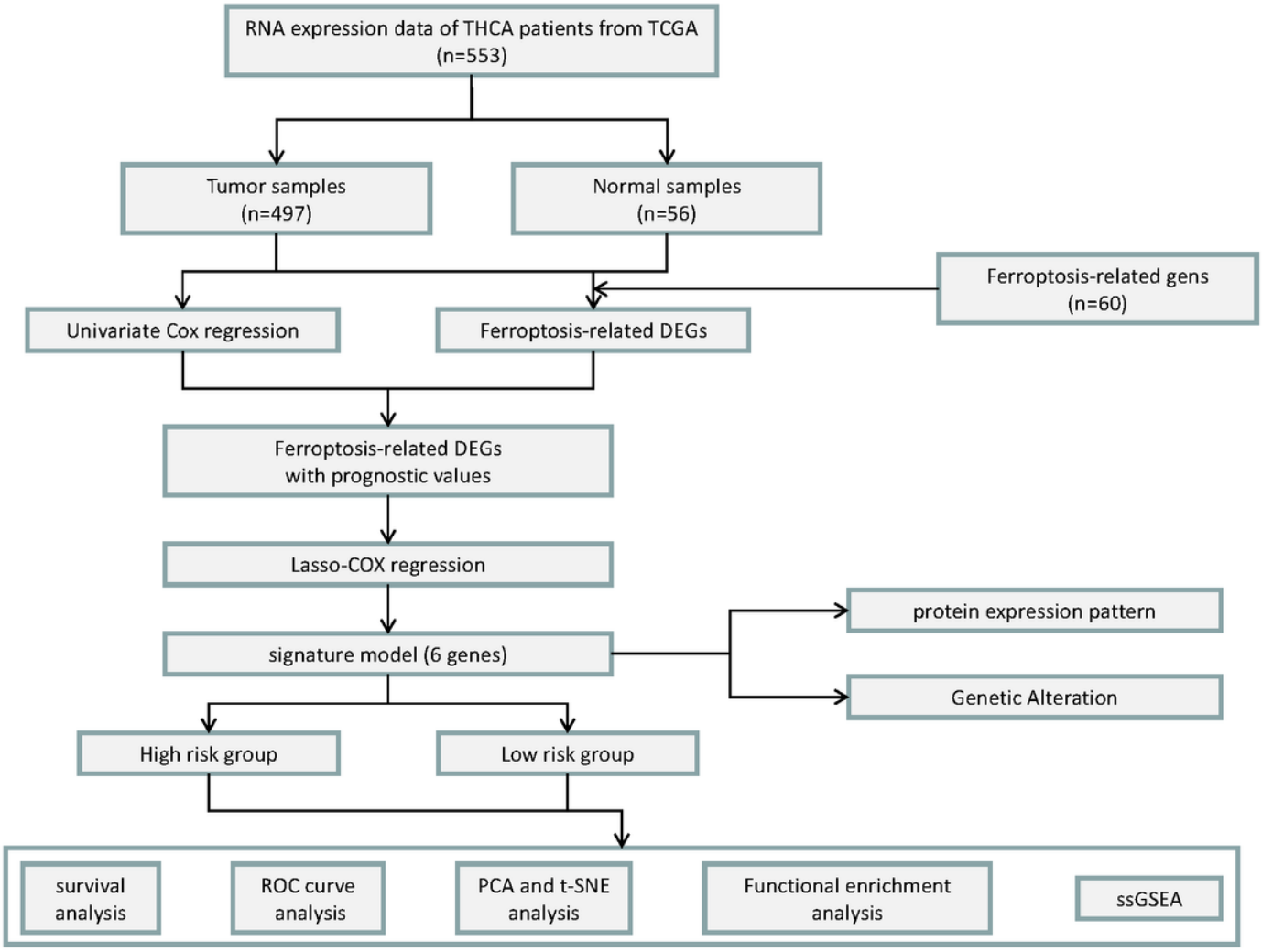

Figure 1

A schematic representation of the study protocol

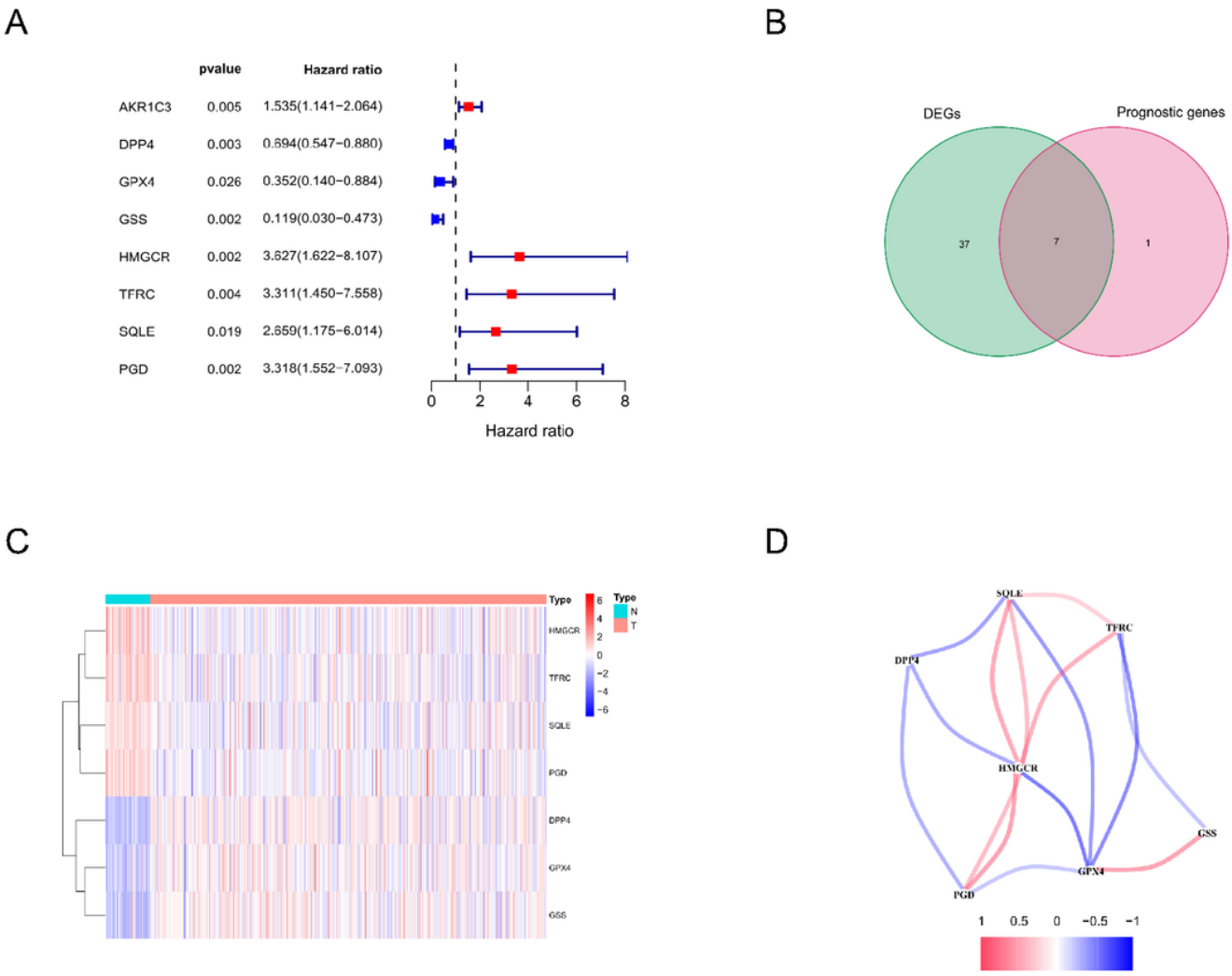

Figure 2

Identification of ferroptosis-related DEGs with prognostic values of THCA in the TCGA cohort a. Univariate Cox regression analysis identified the prognostic genes for OS. b. Venn diagram of the 7 ferroptosis-related DEGs with prognostic values. c. Heat maps displayed the expression of 7 ferroptosis-related DEGs between the different tissue. d. The correlation between 7 ferroptosis-related DEGs.

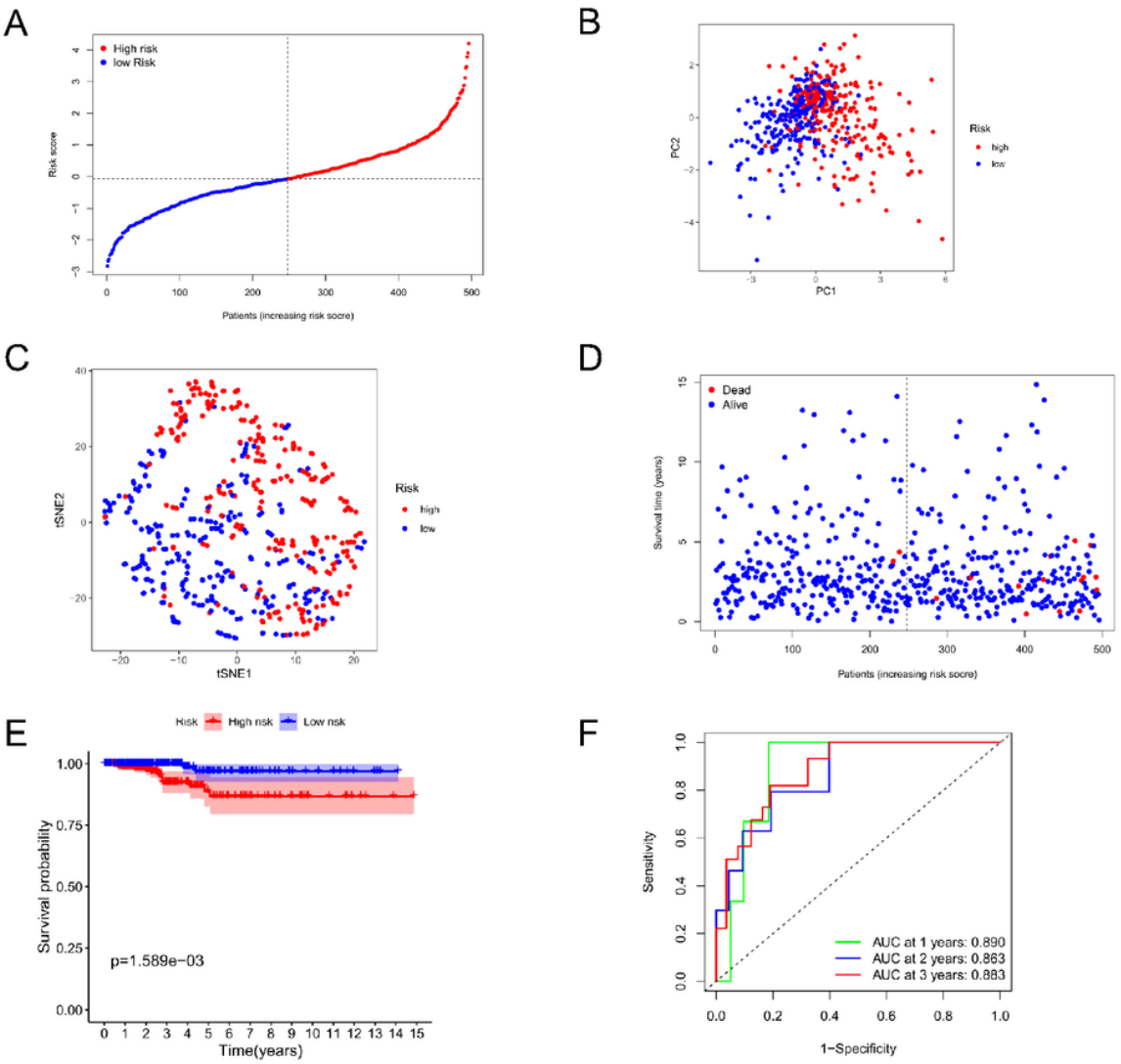

Figure 3

Construction of the prognostic model in the TCGA Thyroid Carcinoma dataset a. Classifying all patients into the high-risk and low-risk groups based on the median risk score. b. PCA analysis of THCA patients in different groups. c. t-SNE analysis of THCA patients in different groups. d. The distributions of the risk scores, survival status and survival time. e. The Kaplan–Meier cumulative curve for the OS of THCA patients in different groups. f. Time-dependent ROC analysis evaluate the prognostic value of the model.

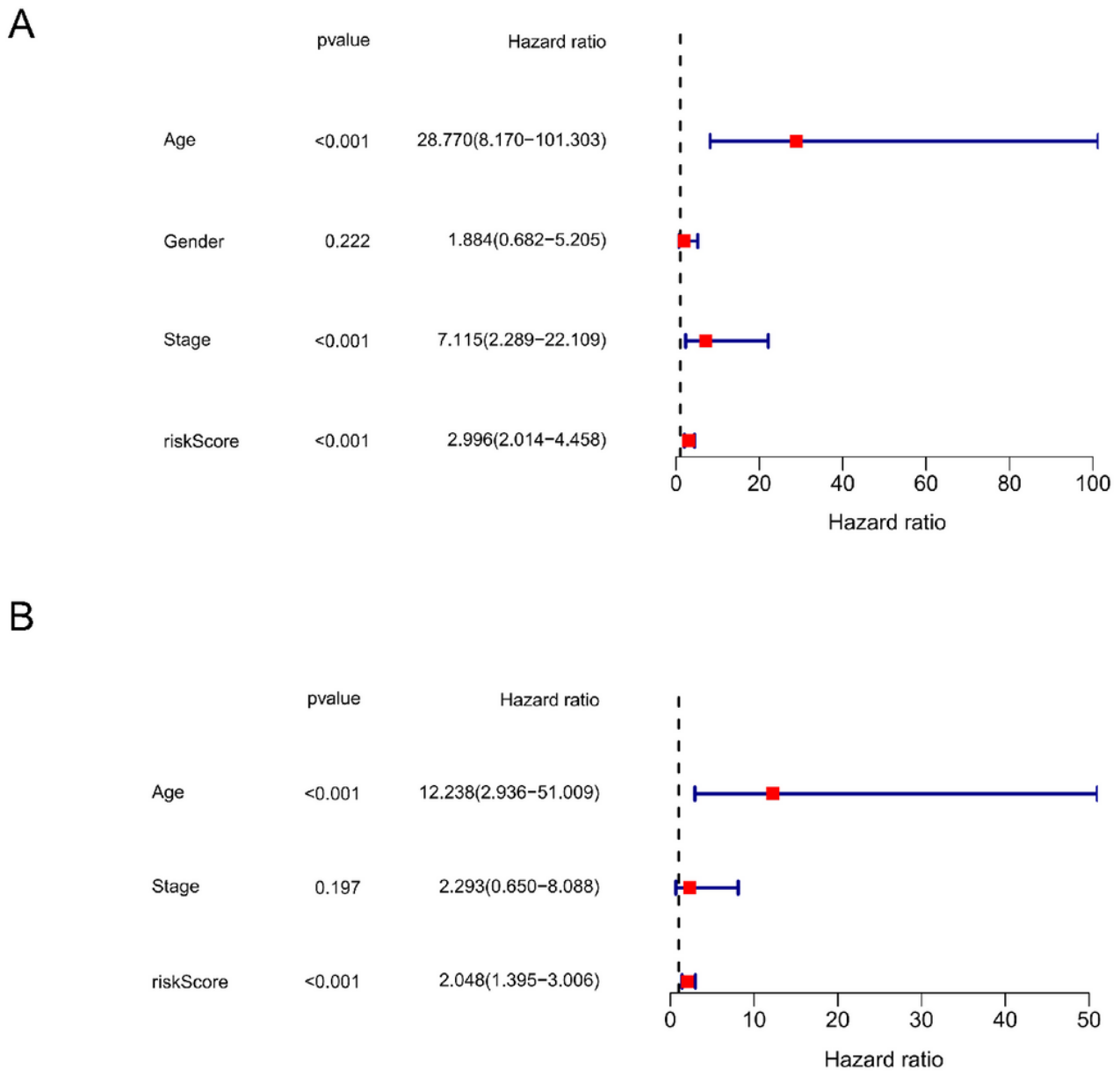

Figure 4

Univariate and multivariate Cox analyses to identify the independent predictive factor for THCA prognosis

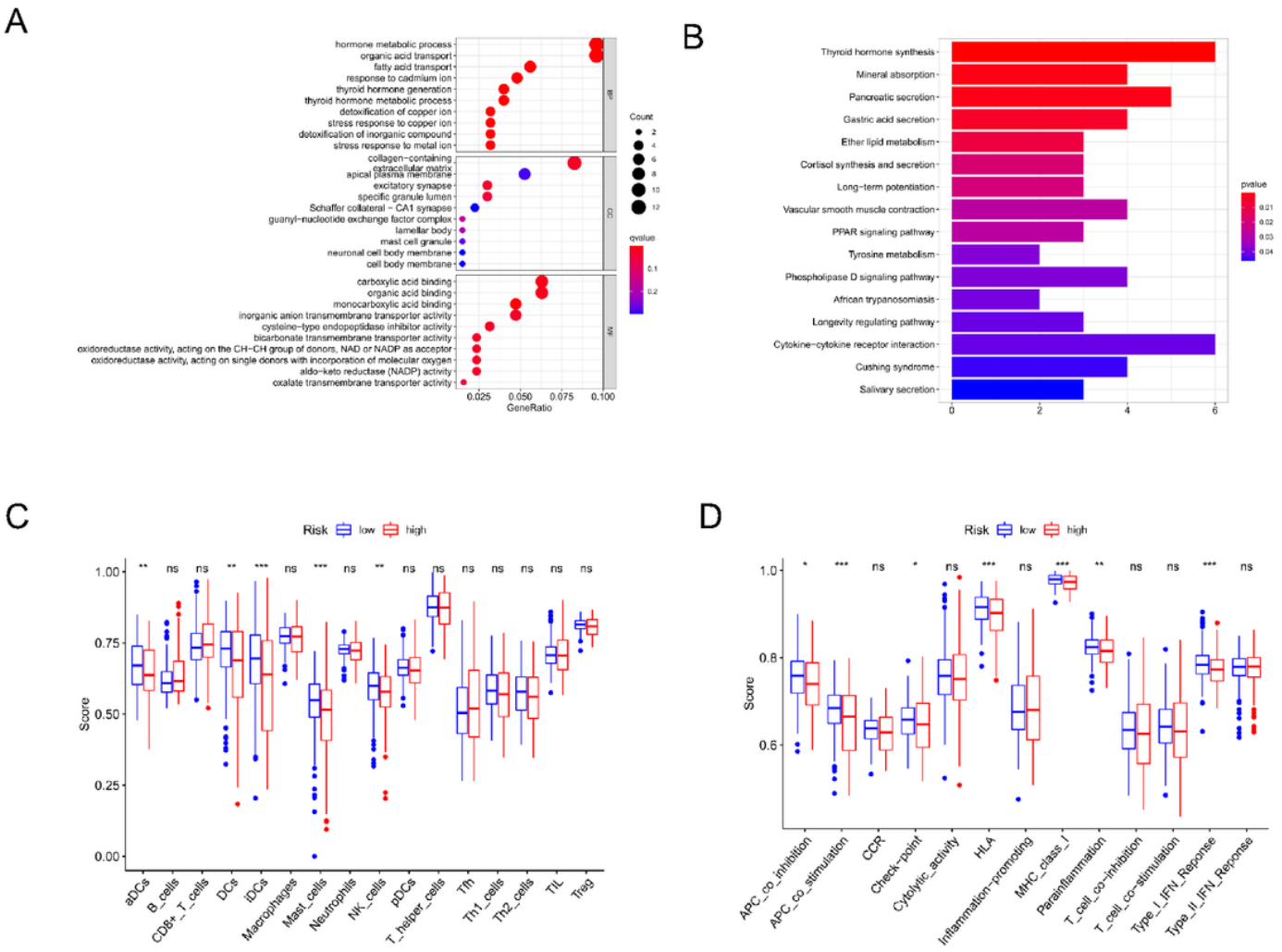

Figure 5

Functional enrichment analysis and immune-related analysis of ferroptosis-related DEGs between the high-risk and low-risk groups a. GO functional analysis of the differentially expressed genes between high-risk and low-risk groups. b. KEGG functional analysis of the differentially expressed genes between high-risk and low-risk groups. c. The ssGSEA scores of 16 immune cells between high-risk and low-risk groups. d. The ssGSEA scores of 13 immune-related functions between high-risk and low-risk groups. (*, P< 0.05; **, P< 0.01; ***, P< 0.001)

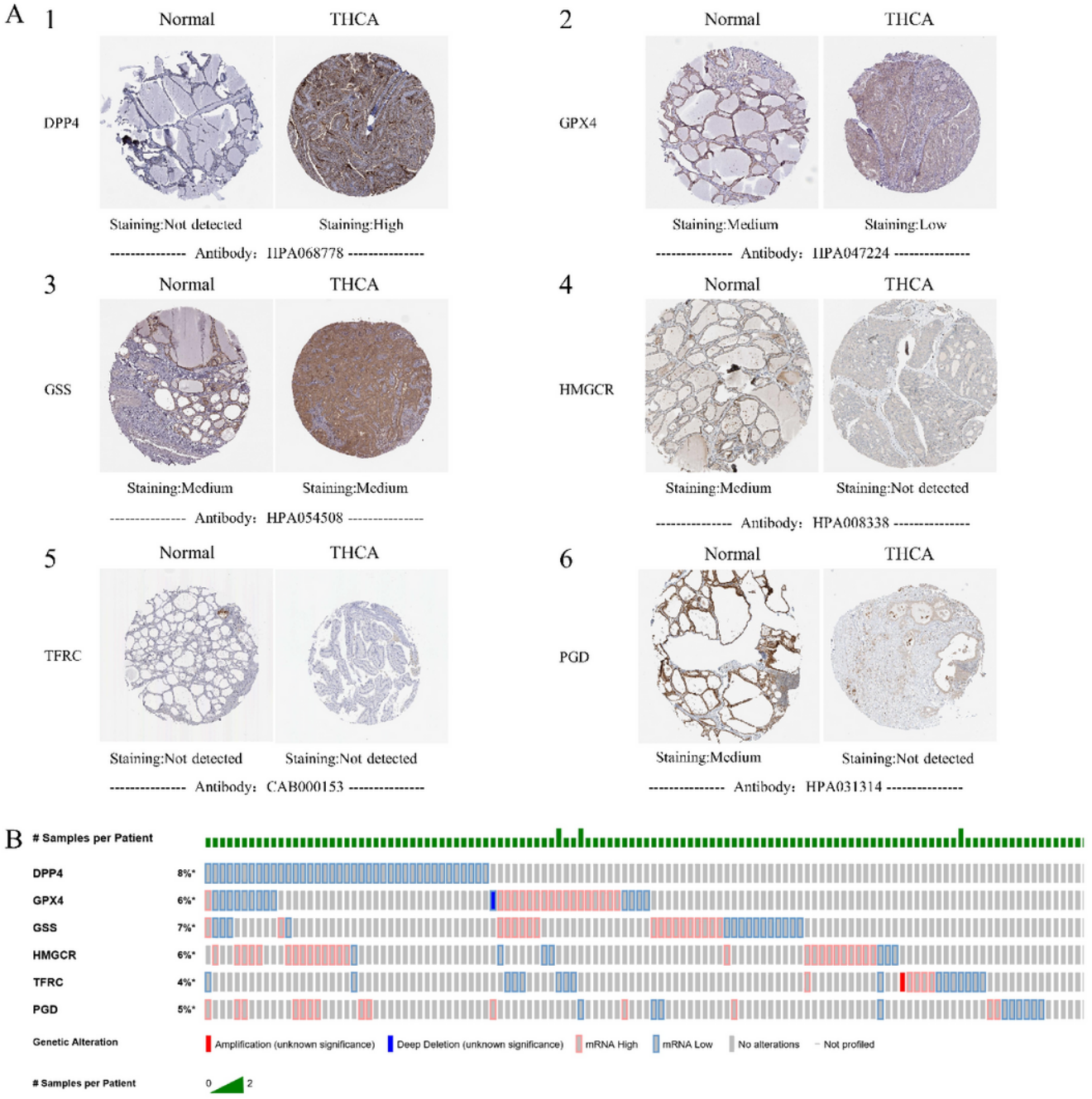

Figure 6

Comprehensive analysis of 6 genes in prognostic signature a. The images shown the protein levels of each gene in normal tissues and the tumor tissues. Immunohistochemistry of the 6 genes in prognostic signature based on the HPA database. b. Genetic alteration of 6 genes in prognostic signature based on the cBioPortal database.

Supplementary Files

This is a list of supplementary files associated with this preprint. Click to download.

- TableS1.xls
- TableS2.xls